Improved state-space models for inference about spatial and temporal variation in abundance from count data

Richard B. Chandler

USGS Patuxent Wildlife Research Center

Laurel, MD 20708

Jeffrey A. Hostetler [*]

Smithsonian Conservation Biology Institute

National Zoological Park, MRC 5503

Washington, DC 20013-7012

October 19, 2012

Abstract

Models of population dynamics play a central role in theoretical and applied ecology where they are used for purposes such as testing hypotheses about density dependence and predicting species' responses to future environmental change or conservation actions. Failure to account for observation error in such models can result in bias, and thus ecologists have increasingly relied on state-space models to directly model both the observation error and the ecological process of interest. Conventional state-space models, however, have three important limitations: (1) the parameters are not identifiable in many common situations, (2) they do not admit spatial variation in population dynamics, and (3) there is no clear interpretation of the observation error. We demonstrate how each of these problems can be resolved using a class of hierarchical models proposed by Dail and Madsen (2011, Biometrics) for spatially-replicated time-series data that attributes observation error to imperfect detection. We expand this class of models to accommodate classical growth models (e.g. exponential, Ricker-logistic, etc ...), zero-inflation, and random effects such as observer-specific detection probabilities. We also present methods for forecasting population size under future environmental conditions. Implementation of these ideas is possible using either frequentist or Bayesian methods, and code to fit these models using the **R** package `unmarked` or **JAGS** is also provided. A simulation study indicated that bias was negligible and coverage nominal for the proposed model extensions. An analysis of data from the North American Breeding Bird Survey highlighted how these methods can be readily applied to existing data, but it also suggested the that precision will be low when direct information about detection probability (such as is collected using distance sampling or replicated counts) is unavailable.

Key words: abundance, Dail and Madsen model, density-dependence, Gompertz-logistic model, immigration, open population point count models, random observer effects, range, Ricker-logistic model, zero-inflated

[*]Contact: `HostetlerJ@si.edu`, +001-202-633-4205

Theoretical ecology requires models of population dynamics for testing hypotheses regarding spatial and temporal variation in abundance. For example, much theoretical work has focused on understanding the importance and existence of phenomenon such as density-dependent population regulation, population cycling, and spatial synchrony (May, 1975; Royama, 1977; Turchin, 1990; Dennis and Taper, 1994; Bjørnstad et al., 1999), and population models are required to evaluate associated hypotheses. In applied contexts, population models are used for estimating extinction probabilities (Schoener and Spiller, 1992; Nadeem and Lele, 2011) and for predicting the effects of future environmental conditions or conservation actions on population size (Jamieson and Brooks, 2004; Hatfield et al., 2012). In order to address these questions, two complicating factors must be confronted when fitting population models to data. First, deterministic models of population dynamics are virtually always inadequate due to process variation, the inherent stochasticity in demographic parameters and environmental conditions (Bjørnstad and Grenfell, 2001; Sæther and Engen, 2002). Second, abundance—the natural state variable in studies of population dynamics—can rarely be observed perfectly in field studies because of observation error, such as imperfect detection (Link and Nichols, 1994; Kery et al., 2009).

State-space models are a widely used approach for studying population dynamics while accounting for process variation and observation error (de Valpine and Hastings, 2002; Buckland et al., 2004; Dennis et al., 2006). Classical state-space models are time-series models in which the true state of the system (e.g. population size during each year) is observed imperfectly. One reason for the widespread adoption of state-space models in ecology is that failure to account for process variation and observation error can bias estimators of abundance and population growth parameters. For instance, the strength of density dependence will be over-estimated if observation error is ignored (Link and Nichols, 1994; Shenk et al., 1998).

A simple state-space models can be described as follows. Let N_t be the abundance of a species during year t, for $t = 1, \ldots, T$, and let X_t be the observed data, which differs from N_t due to observation error, a random effect denoted ζ_t. Temporal variation in N_t is modeled using a population growth model, $\mu(N_{t-1})$ and random process variation denoted $\grave{o}_t$. The growth model may be density-dependent, as in the case of the Ricker-logistic model, or it might be density-independent, such as when growth is exponential. The full model can now be written as:

$$N_1 = X_1 \tag{1a}$$
$$N_t = \mu(N_{t-1}) + \grave{o}_{t-1} \quad \text{for } t = 2, \ldots, T \tag{1b}$$
$$X_t = N_t + \zeta_t \qquad\quad \text{for } t = 1, \ldots, T \tag{1c}$$

where $\grave{o}_t$ is the random effect allowing for process variation unaccounted for by the deterministic model. In classical state-space models, the two sets of random effects are assumed to be i.i.d. Gaussian deviates: $\grave{o}_t \sim \mathrm{N}(0, \sigma)$ and $\zeta_t \sim \mathrm{N}(0, \tau)$. It is also standard practice to ignore process variation associated with N_1, as indicated by Eq 1a. Alternatively, the population is assumed to be at equilibrium such that the N_1 can be regarded as an outcome of the equilibrium distribution.

Even though state-space models such as that shown in Eq. 1 are among the most widespread approaches for modeling population dynamics using time-series data, several problems are evident. Namely, (1) time-series data and the underlying abundance parameters of interest are typically integer-valued, as in the case of count data, raising concerns about the use of Gaussian distribution for the random effects, (2) the model for observation error has little biological basis, (3) spatial variation in abundance is not allowed, and (4) some of the parameters of the model are not estimable. We briefly discuss each of these points before describing a general approach to resolving these shortcomings.

Use of the Gaussian distribution for modeling random process variation and observation error is motivated by convenience rather than biology. Specifically, the Gaussian assumptions allow for parameter estimation using the Kalman filter (Dennis et al., 2006), which is much more computationally efficient than estimation methods when random effects are not Gaussian distributed (de Valpine and Hastings, 2002). The problem with this is that it allows for negative and non-integer values of the state-variable, which is inconsistent with the observed data, and may result in implausible predictions. Transforming the count data and the underlying abundance variables do little to resolve these issues (O'Hara and Kotze, 2010).

Another problem with standard state-space models is that the observation error has no clear interpretation. The use of a mean zero Gaussian distribution implies that X_t will be higher than N_t as often as it is lower than N_t. It is hard to identify a mechanism that would cause such symmetric errors. A more likely form of observation error, and one that has been recognized for well over a century, results from failing to detect individuals that are present. Imperfect detection may be attributable to characteristics of the species under study, such as its elusiveness, or to the failings of the ecologist collecting the data in the field. Although a vast number of methods have been devised for accounting for this form of observation error, rarely have these methods been integrated into state-space models (but see Buckland et al., 2004).

A more serious problem than the ones associated with the Gaussian assumptions is that the parameters of the simple state-space models such as Eq 1 are not identifiable in many circumstances (Polansky et al., 2009). Recall that the Eq. 1 did not specify distributions for N_1; however, N_1 is a random variable and hence there is uncertainty that should be accounted for. To be more specific, a fully-specified state-space model requires at least three probability distributions, which we represent using bracket notation (i.e., $[Y|\Omega]$ is interpreted as the probability distribution of the random variable Y given the parameter Ω). The three probability distributions required for a state-space model are:

$$[N_1|\boldsymbol{\theta}] \tag{2a}$$

$$[N_t|N_{t-1}, \boldsymbol{\Theta}] \quad \text{for } t = 2, \ldots, T \tag{2b}$$

$$[X_t|N_t, \boldsymbol{p}] \qquad \text{for } t = 1, \ldots, T \tag{2c}$$

where $\boldsymbol{\theta}$ are the process variation parameters for the initial state, $\boldsymbol{\Theta}$ are the process variation parameters influencing how abundance changes over time, and $\boldsymbol{p}$ are the observation error parameters. As mentioned previously, Eq. 2b and Eq. 2c are assumed to be Gaussian in classical state-space models, but what should be the distribution for Eq. 2a? And how could $\boldsymbol{\theta}$ be estimated given that there is only a single observation available? Often, these problems are simply assumed away. For example, sometimes researchers assume that there is no process variation in the first year, although this seems unjustified. Alternatively, the population may be assumed to be at equilibrium such that the expected value of N_t is constant through time. Although this makes the parameters $\boldsymbol{\theta}$ identifiable, assuming equilibrium defeats the objective of many studies of population dynamics, namely determining why a population varies over time.

A fourth problem with these models is that they do not admit spatial variation. This reduces the scope of the inferences that can be drawn from the models and it ignores the importance of space in population regulation.

Several extensions of state-space models have been proposed to overcome the limitations described above. de Valpine and Hastings (2002) and Kery et al. (2009) described methods for fitting models with non-Gaussian distributions for the process and observation errors. Observation models with more intuitive interpretations, such

as those that explicitly model detection probability, have been proposed by Kery et al. (2009). Lele et al. (1998) and Kery et al. (2009) developed models allowing for inference about spatial and temporal variation in abundance, and their developments also resolved the problems of non-identifiability for the parameters of the initial state at time $t = 1$. Of these extensions, only the work by Kery et al. (2009) addressed several of these limitations simultaneously. However, their model did not include serial dependence, which is a hallmark of population models. This limits the utility of their model for making inferences about explicit population processes.

In this paper, we focus on the model of Dail and Madsen (2011, henceforth the DM model;) that simultaneous resolves each of the aforementioned problems with traditional state-space models, and is designed for simple countdata. In the following section, we describe the DM model in its original form and explain how it resolves each of the deficiencies with standard state-space models. In Section 3, we extend the model to accommodate classical models of population growth and to handle several features common to ecological time-series. Specifically, we describe methods for accommodating excess zeros and nuisance variables such as random observer effects. Both frequentist and Bayesian methods of inference are discussed, and code for fitting models is presented in the appendices. In Section 4, we evaluate the performance of the model extensions using a simulation study and by analyzing data from the North American Breeding Bird Survey (BBS), one of the most spatially and temporally extensive sets of count data on vertebrate populations (Robbins et al., 1986). The overarching aim of the paper is to provide ecologists with flexible and accessible means of addressing important questions related to the variation of abundance in space and time.

1 The Dail-Madsen Model

The DM model is an extension of the N-mixture model (Royle, 2004), which allows for inference about spatial variation in abundance when individuals cannot be detected with certainty. To estimate both abundance parameters and parameters of the detection process, the original N-mixture model uses replicate observations at each site, which are collected during sufficiently short time intervals such that the population can safely be assumed to be closed with respect to births, deaths, and movement. The DM model relaxes this closure assumption and includes explicit parameters describing population change over time.

1.1 The Data

The DM model requires count data collected at R sites, each of which is surveyed on T primary sampling periods. A site is ideally a well-defined region of a study area, such as a wetland or a patch of early-successional habitat, although it could be an arbitrarily defined region such as a randomly located survey plots. The time frame of the study is arbitrary, but in general it will be sufficiently long to allow for temporal variation in abundance. For instance, a primary sampling period could be a one month long breeding season, which could be surveyed once per year for T years. If the a site is surveyed on J occasions during a primary period, these are called secondary sampling occasions. In the case where no secondary sampling was conducted, i.e. $J = 1$, let $X_{it} : i = 1, \ldots, R; t = 1, \ldots, T$ denote the count data at site i and primary period t. If secondary sampling periods were used, an extra dimension is added so that we have $X_{ijt} : j = 1, \ldots, J$. Typically, we X_{it} will be lower than the actual quantity of interest, abundance, denoted N_{it}. In cases where

detection probability is perfect, abundance is observed directly such that $X_{it} \equiv N_{it}$.

1.2 The Original Formulation of the Model

As with traditional state-space models, the DM model includes the three condition-ally related processes shown in Eq. 2, which correspond to (1) initial abundance, i.e. the abundance at site i during the first primary period, denoted (2) abundance at time t (for $t > 1$) which depends upon abundance at $t - 1$, and (3) the detection pro-cess (Dail and Madsen, 2011). The first two processes describe the state process—the variation in abundance in space and time. The third process simply describes the the relationship between abundance and the observed count data.

1.2.1 Initial abundance

Recall that conventional state-space models assume that the distribution for the initial time period, $[N_1|\boldsymbol{\theta}]$, is either the equilibrium distribution, or has zero variance. In contrast, Dail and Madsen (2011) proposed modeling N_{i1} as either a Poisson or negative binomial random variable:

$$N_{i1} \sim \text{Pois}(\Lambda)$$
$$\text{or}$$
$$N_{i1} \sim \text{NB}(\Lambda, \alpha) \tag{3}$$

where Λ_i is the expected abundance at site i during year 1. The Poisson distribution assumes that the mean of N_{i1} is equal to its variance, whereas the negative binomial distribution allows the variance to be greater than the mean with the amount of overdispersion determined by the parameter α. In the Poisson case, the equivalent expression of $[N_1|\boldsymbol{\theta}]$ (Eq. 2a) is

$$[N_{i1}|\Lambda] = \frac{\Lambda^{N_{i1}} e^{-\Lambda}}{N_{i1}!}. \tag{4}$$

Regardless of the specified distribution, the model for initial abundance has two distinguishing features. First, it provides a mechanism for characterizing spatial variation in abundance. For instance, one might consider the influence of some en-vironmental covariate (x_i) on abundance using a log-linear model such as $\log(\Lambda_i) = \beta_0^\Lambda + \beta_1^\Lambda x_i$. The second important point is that the spatial replicates resolve the prob-lem of parameter non-identifiability that are common to standard state-space models because, as demonstrated by Royle (2004), process variation and observation error can be estimated from spatially-replicated count data. Hence, the first component of the model addresses both the issues of spatial inference and parameter identifiability discussed previously.

1.2.2 Abundance in subsequent time periods

The DM model assumes that abundance in time t is a function of abundance in time $t - 1$, i.e. abundance at each site evolves as a first order Markovian process, although higher order processes are also possible. Dail and Madsen (2011) considered several models to describe the temporal dynamics; however, in each case they modeled N_t as the sum of two random variables: S_{it}, the number of indivduals surviving from $t - 1$ and not emigrating; and G_{it} the number of new individuals entering the population.

Their most general model was

$$
\left.
\begin{aligned}
S_{it}|N_{it-1} &\sim \mathrm{Bin}(N_{it-1}, \omega) \\
G_{it}|N_{it-1} &\sim \mathrm{Pois}(\gamma(N_{it-1})) \\
N_{it} &= S_{it} + G_{it}
\end{aligned}
\right\} \quad \text{for } t = 2, \ldots, T \tag{5}
$$

where ω is the apparent survival probability and γ is the recruitment rate (which can depend on N_{it-1}). Dail and Madsen (2011) proposed three models for γ: the constant model, $G_{it} \sim \mathrm{Pois}(\gamma)$ where recruitment does not depend on N_{it-1}, and which simulates a "propagule rain" of new individuals; the autoregressive model, $G_{it} \sim \mathrm{Pois}(\gamma(N_{it-1}))$, which simulates geometric or density independent growth; and the "no-trend" model, $\gamma = (1-\omega)\Lambda$, which keeps expected abundance constant over time. As before, covariates of ω and γ can be easily accommodated, for example using logit- and log-linear models respectively.

To make the connection between conventional state-space models and the DM model, we need to replace $[N_t|N_{t-1}, \boldsymbol{\Theta}]$, Eq. 2b, with an expression derived from Eq. 5. This requires summing over all possible values of S and G, which is accomplished using the discrete convolution:

$$
[N_{it}|N_{it-1}, \omega, \gamma] = \sum_{S_{it-1}=0}^{\min(N_{it}, N_{it-1})} \binom{N_{it-1}}{S_{it-1}} \omega^{S_{it-1}} (1-\omega)^{N_{it-1}-S_{it-1}} \times \frac{\gamma^{N_{it}-S_{it-1}} e^{-\gamma}}{(N_{it}-S_{it-1})!} \tag{6}
$$

where here we assumed no dependence of γ on N_{it-1}.

In the absence of movement, ω is exactly the probability of surviving from year t to $t-1$, and γ is the per-capita birth rate (under the geometric growth model). This ability to directly estimate demographic parameters from simple count data is one of the DM model's most appearling features. However, in the more common scenario when immigration and emigration occur, ω and γ no longer can be interpreted as vital rates. Rather, ω is the probability of surviving and not emigrating, and γ is the sum of the birth rate and the immigration rate, i.e. the recruitment rate. In such cases, we propose replacing Eq. 5 with standard population models.

1.2.3 Observation process

Eqs. 3 and 5 fully specify the state model, i.e. the model for abundance dynamics. This state model has allowed us to replace the initial abundance distribution and transition models of conventional state-space models, with alternatives that (1) allow for modeling spatial variation in abundance, (2) respect the discrete nature of the counts, and (3) have parameters that are estimable. The one remaining task is to replace the observation model $[X_t|N_t, \boldsymbol{p}]$ (Eq. 2c) with one that can be more easily interpreted. The observation model assumes that individuals are missed due to imperfect detection. The simplest model for imperfect detection, and the one considered in the original formulation, is

$$
X_{it} \sim \mathrm{Bin}(N_{it}, p) \tag{7}
$$

or equivalently,

$$
[X_{it}|N_{it}, \boldsymbol{p}] = \binom{N_{it}}{X_{it}} \boldsymbol{p}^{X_{it}} (1-\boldsymbol{p})^{N_{it}-X_{it}}. \tag{8}
$$

Under this model, $\boldsymbol{p}$ are interpretted as detection probability parameters...

The entire model can now be written:

$$
\begin{aligned}
N_{i1} &\sim \text{Pois}(\Lambda) \\
S_{it}|N_{it-1} &\sim \text{Bin}(N_{it-1}, \omega) \\
G_{it}|N_{it-1} &\sim \text{Pois}(\gamma(N_{it-1})) \\
N_{it} &= S_{it} + G_{it} \\
X_{it} &\sim \text{Bin}(N_{it}, p)
\end{aligned}
\tag{9}
$$

2 Statistical Inference

2.1 Maximum likelihood

Maximum likelihood estimation of parameters in models with discrete random effects requires removing them by summation. For Markovian models, this can be done recursively, making the likelihood tractable. A general expression of the likelihood can be written:

$$
\mathcal{L}(\Lambda, \boldsymbol{\Theta}, p|\{X_{it}\}) =
\prod_{i=1}^{R} \left\{ \sum_{N_{i1}=0}^{\infty} [X_{i1}|N_{i1}, p][N_{i1}|\Lambda] \left\{ \sum_{N_{i2}=0}^{\infty} \cdots \sum_{N_{iT}=0}^{\infty} [X_{it}|N_{it}, p][N_{it}|N_{it-1}, \boldsymbol{\Theta}] \right\} \right\}
\tag{10}
$$

where ∞ is replaced by a finite upper bound K, which should be high enough such that the MLEs are not affected by increasing it further. This likelihood can be maximized numerically using the **R** package `unmarked` (Fiske and Chandler, 2011). Examples are given in the Appendix.

2.2 Bayesian inference

Bayesian inference has several appealing features. First, it allows direct probability statements to be made about a hypothesis given data. [EXPLAIN POSTERIORS AND PRIORS] Second, Bayesian methods offer straight-forward approaches for combine data from multiple sources or use existing estimates of parameters as prior distributions. In practice, simulation methods such as Markov chain Monte Carlo (MCMC) are used to simulate the posterior distributions. Although MCMC can be slow, our experience is that it may actually converge faster than the amount of time required to maximize the likelihood shown in Eq.10, especially when the upper bound of the summation must be high, e.g. $K > 200$. Furthermore, MCMC may be the only possible option for estimating parameters using some of the extensions described below, such as allowing for additional random effects.

Writing custom MCMC algorthims is often tedious and foreign to ecologists, but software packages such as **WinBUGS** and **JAGS** overcome the technical difficulties by allowing users to specify the model using a simple symbolic descriptions. For example here is **BUGS** code for the "geometric" model described shown in Eq. 1.2.3:

```
model {
lambda ~ dunif(0, 5)
omega ~ dunif(0,1)
gamma ~ dunif(0, 10)
p ~ dunif(0,1)
for(i in 1:nSites) {
```

```
    N[i,1] ~ dpois(lambda)
    y[i,1] ~ dbin(p, N[i,1])
    for(t in 2:nYears) {
      S[i,t-1] ~ dbin(omega, N[i,t-1])
      G[i,t-1] ~ dpois(gamma*N[i,t-1])
      N[i,t] <- S[i,t-1] + G[i,t-1]
      n[i,t] ~ dbin(p, N[i,1])
      }
    }
}
```

3 Model Extensions

3.1 Population growth models

Although partitioning population growth into survival and recruitment is ideal in terms of providing a mechanistic description of population dynamics, it is not always possible using simple count data, especially when the sites are not closed with respect to immigration and emigration. If the mechanistic model must be sacrificed, we suggest replacing it with classical population growth models that have a long history in ecology. The simplest of which is the exponential growth model: $f(N_{it-1}) = N_{it-1}e^r$ where r is the intrinsic rate of increase. Although demographic and environmental stochasticity in r could be modeled as functions of covariates or random effects, a simpler way of allow for stochasticity is to regard N_{it} as a Poisson random variable, simplifying Eq. 5 to:

$$N_{it} \sim \text{Pois}(\exp(r)N_{it-1}). \tag{11}$$

This, like the autoregressive version of the model, is a variant on a simple density-independent exponential model of population growth. Density-dependent versions of the model are also possible. For example:

$$N_{it} \sim \text{Pois}(N_{it-1}\exp(r(1 - N_{it-1}/K)) \tag{12}$$

where K is the stable equilibrium of the population and r is the instantaneous population growth rate at low population densities, and both parameters are constrained to be positive. This is a stochastic version of the Ricker-logistic population growth model (Ricker, 1954). We also implemented a modified Gompertz-logistic density-dependent model (Hart and Gotelli, 2011):

$$N_{it} \sim \text{Pois}(N_{it-1}\exp(r(1 - \log(N_{it-1} + 1)/\log(K + 1))) \tag{13}$$

Here the interpretations of r and K are similar to in the Ricker-logistic model.

Because a single Poisson distribution controls the distribution of N_{it} in each of these models, the discrete convolution used by Dail and Madsen (2011) is not required, speeding up processing time.

```
model {
lambda ~ dunif(0, 5)
r ~ dunif(-5, 5)
p ~ dunif(0,1)
for(i in 1:nSites) {
  N[i,1] ~ dpois(lambda)
  y[i,1] ~ dbin(p, N[i,1])
```

```
  for(t in 2:nYears) {
    mu[i,t-1] = N[i,t-1]*exp(r)
    N[i,t] ~ dpois(mu[i,t-1])
    n[i,t] ~ dbin(p, N[i,1])
    }
  }
}
```

3.2   Immigration models

The autoregressive, exponential, Ricker-logistic, and Gompertz-logistic versions of
the DM models all share a common feature (or bug): once the population at a
site reaches 0, it must remain at 0. This is because all contributions to population
growth are local in these models. We generalized each these models that include
both internal and external (immigration) contributions to population growth. The
exponential plus immigration model is:

$$N_{it} \sim \text{Poisson}(\exp(r)N_{it-1} + \iota) \tag{14}$$

where ι represents the immigration rate, and is constrained to be positive (this is
equivalent to separate Poisson processes for growth and immigration). This model is
close to the constant DM model (Eq. 5), with $\exp(r)$ instead of ω and ι instead of γ,
except that the first process is Poisson distributed instead of binomial. The autore-
gressive, Ricker-logistic, and Gompertz-logistic models can be extended to allow for
immigration in the same way.

   We have implemented all preceding models in a maximum likelihood framework
by extending the `unmarked` package (Fiske and Chandler, 2011) in **R** (R Development
Core Team, 2012).

3.3   Excess zeros

Dail and Madsen (2011) suggested two distributions for modeling initial abundance:
Poisson and negative binomial. We have extended their model to include another
distribution, the zero-inflated Poisson. This could be useful when, for example, one is
modeling the abundance of several bird species with the same set of BBS routespoint
count surveys for all species, but this set includes routes sites outside the range of
some of the bird species. The distribution of initial abundances can be represented
as:

$$N_{i1} \sim \begin{cases} 0 \text{ with probability } \psi \\ \Lambda \text{ with probability } (1-\psi) \end{cases} \tag{15}$$

where ψ represents the proportion of extra zeros.

   These models allow three sources of zero counts by observers: a species was at
a route but not detected; the route was within the species' range but there were
no birds at that site in that year; and the route was outside the species' range.
Furthermore, detection, abundance, and zero-inflation can be modeled separately as
functions of different (or the same) covariates. For example, detection of species x at
site y in year z might depend on wind speed, abundance on forest type and weather,
and zero-inflation upon elevation and climate. This approach combines elements of
occupancy modeling (MacKenzie et al., 2006) and abundance modeling.

   The zero-inflated Poisson distribution can be applied to not only initial abundance
but also to recruitment and population growth terms. For example, the recruitment

term of the constant DM model (Eq. 5) can be modified as follows:

$$G_{it} \sim \begin{cases} 0 \text{ with probability } \psi \\ \text{Poisson}(\gamma) \text{ with probability } (1 - \psi) \end{cases} \tag{16}$$

We have implemented zero-inflated dynamics in the Bayesian framework using program JAGS (Plummer, 2003, version 3.2.0).

3.4 Environmental and demographic stochasticity

Even though the DM model is conceptually very simple, even in its most stripped down form it includes many random effects (the N's) making it challenging to compute the likelihood or implement MCMC algorithms. Nonetheless, in some cases additional random effects may be of interest. For example, in conventional state-space models, demographic stochasticity is often modeled as $r_t \sim \text{Norm}(\mu_r, \sigma_r)$.

3.5 Random effects of observers

Variation in detection probability among observers is another source of random variation that may need to be accounted for applying the DM model. For example, differences in observers' ability to see, hear, or identify birds has long been recognized as a potential source of error in avian point count surveys such as the BBS (Robbins et al., 1986; Diefenbach et al., 2003; Sauer et al., 1994; Alldredge et al., 2007; Campbell and Francis, 2011). Estimating a separate detection probability for each observer can be difficult and reduces one's ability to estimate the quantities of interest. This problem is compounded by the fact that observers differ greatly in the number of surveys they have run (so that many observers' separate detection probabilities could not be accurately estimated).

Current BBS trend estimators deal with this problem by treating observer identity as a random (as opposed to a fixed) effect (Link and Sauer, 2002; Sauer and Link, 2011). This allows observer-specific differences in detection probability, but assumes that observers are selected at random from a pool of potential observers. Models that contain both random and fixed effects are referred to as mixed models. Often in mixed models (as in this case), the random effect is modeled not because it of interest in itself, but to avoid bias in the estimates of the fixed effects.

To include random observer effects in DM models and these extensions, Eq. 7 can be modified to:

$$X_{ijt} \sim \text{Bin}(N_{it}, p_j)$$
$$\text{logit}(p_j) \sim \text{Normal}(\mu_p, \sigma_p) \tag{17}$$

where X_{ijt} is the number of bird recorded at site i by observer j in year t, p_j is observer-specific detection probability, μ_p is the mean detection probability (on the logit scale), and σ_p is the standard deviation of the random observer effects (also on the logit scale). We have implemented random observer effects in the Bayesian framework using program **JAGS** (Plummer, 2003, version 3.2.0) with the **R** package `rjags` (Plummer, 2011; R Development Core Team, 2012) interface.

3.6 Forecasting Future Population Size

State-space models allow for inference about future population size, a critical component of population viability analysis as well as conservation planning. Let N_t^+ denote population size at some future point in time and $[N_t^+]$ denote the probability

distribution for this random variable. If we can specify this distribution, we can make statements about the probability that $N_t^+ = k$ where k is any possible population size including zero.

The classical approach to computing $[N_t^+]$ is based upon Empirical Bayes methods. Note that neither Empiriis not actually a Bayesian method, it is used to estim. We take the parameter estimates and plug them back in.... For example to obtain the posterior distribution for $[N_{i1}]$

$$[\hat{N}_{i1}] = \frac{[N_{i1}|\hat{\Lambda}][X_{i1}|N_{i1},\hat{p}]}{\sum_{N_{i1}=0}^{K}[N_{i1}|\hat{\Lambda}][X_{i1}|N_{i1},\hat{p}]} \tag{18}$$

Once we have estimated the posterior distribution for the first time period, we can then proceed to estimate the posterior distribution for subsequent time periods using recursion.

$$[\hat{N}_{it}] = \frac{[N_{it}|N_{it-1},\hat{\boldsymbol{\Theta}}][X_{it}|N_{it},\hat{p}]}{\sum_{N_{it}=0}^{K}[N_{it}|N_{it-1},\hat{\boldsymbol{\Theta}}][X_{it}|N_{it},\hat{p}]} \tag{19}$$

Note that when X_{it} is not observed, including for future time periods, the distribution $[X_{it}|N_{it}]$ is taken to be uniform such that it has no influence on the posterior. In other words, the posterior for years with no observed data is determined entirely by the estimated posterior from the previous year and the population dynamics parameters.

If covariates of the dynamics parameters are present, the problem becomes much harder because, to fully account for uncertainty, we need a model for the future values of the covariates as well. When the covariates are continuous, this requires integrating over their possible values, which becomes very challenging computationally. Indeed, simulation methods such as MCMC are the only viable options when numerous covariates are present, which will often be the case in many ecological studies.

Relative to the computational challenges associated with the empirical Bayes methods, the Bayesian approach is much more easy to implement, especially since MCMC will be generally be relied upon in the first place. Furthermore, because population size at any future point in time is regarded as an unknown parameter like any other, computing the posterior distribution of N_t^+ requires no additional steps in MCMC algorithm, other than formally stating that the count data are "missing" in future years. An example of this is provided in the appendix.

4 Applications

4.1 Simulation Study

We simulated data for 100 sites over 40 years. All simulations assumed initial abundance was Poisson distributed and no covariates affected initial abundance, dynamics, or detection probability. Our first series of simulations assumed dynamics were exponential. We ran 1000 simulations for each combination of low, medium, and high $\Lambda \in \{1, 5, 10\}$, $r \in \{-0.005, 0, 0.005\}$, and $p \in \{0.05, 0.25, 0.5\}$. Our second series of simulations changed dynamics to the Ricker-logistic model. We used an initial abundance of 10 and a detection probability of 0.25, and simulated low, medium, and high values of equilibrium abundance and maximum growth rate, each with 1000 simulations (Table 1; 9 total combinations). Our third series of simulations was based on the Ricker-logistic + immigration dynamics model; here we fixed all parameters the same as the Ricker-logistic model (with r = 0.05 and K = 10) and simulated low, medium, and high values of immigration rate with 1000 simulation each (Table 1).

11

We estimated the parameters for each simulation using the same initial abundance (Poisson) and dynamics models as were simulated, implemented in the unmarked library in **R**. When run in a maximum likelihood framework, these models require a maximum abundance to integrate over (Royle, 2004; Dail and Madsen, 2011); we used 200. We report bias of estimates, root mean squared error, and coverage (percentage of 95% confidence intervals for parameters that overlap the true values).

4.2   Analysis of Breeding Bird Survey Data

We applied these models to North American Breeding Bird Survey (BBS) data from 1966-2010 for two species in the bordering US states Maryland and Virginia. For our focal species, we selected ovenbirds (*Seiurus aurocapilla*), an abundant and widespread forest breeding migrant with a stable or increasing trend in the region (CITE) and golden-winged warblers (*Vermivora chrysoptera*), which only breeds in the western parts of these states and has been declining in the region (CITE).

The BBS is an annual roadside survey implemented by trained observers in the United States and Canada. An observer conducts 50 3-minute point counts, with 400 m radiuses and 0.8 km apart from each other along a 39.4 km route. We only used data marked as acceptable for use in the annual BBS analysis (Sauer et al., 1994). We summed the total birds of each species seen on each route and year and used the routes (rather than the individual stops) as our sites. Strong winds can interfere with point count observers' ability to hear birds (Simons et al., 2007); we tested the effects of wind speed on detection probability. BBS volunteers record wind conditions at the beginning and end of each route on the Beaufort Scale (Robbins et al., 1986, start and end wind). When start or end wind was not recorded we imputed those values with the start or end mean. We took the mean of start and end wind for each route and put this average wind scale value into four categories: $0 \leq \text{wind} < 1$; $1 \geq \text{wind} < 2$; $2 \leq \text{wind} < 3$; and $\text{wind} \geq 3$ (maximum of 3.5). Following Link and Sauer (2002), we also included the first time an observer ran a route as a predictor variable for detection probability.

We ran a series of maximum-likelihood based models for each species, and then a series of Bayesian models. We started by testing three models of initial abundance (Poisson, negative binomial, and zero-inflated Poisson) with exponential dynamics (Eq. 11) and no covariates. We selected the minimum Akaike's Information Criterion (AIC) model from that set to test three additional models for p: wind, first, and wind + first. We selected the minimum AIC model from that set to test eight additional models of dynamics: constant, autoregressive, Ricker-logistic, Gompertz-logistic, autoregressive + immigration, exponential + immigration, Ricker-logistic + immigration, and Gompertz-logistic + immigration. As above, these models require a maximum abundance to integrate over when run in a maximum likelihood framework; we used 600 for ovenbirds and 350 for golden-winged warblers.

We ran the top ranked models from the maximum likelihood analyses in a Bayesian framework. We added random observer effects and, where appropriate, zero-inflated dynamics. We used non-informative priors. We tested for lack of convergence using 5 Markov chains for each model (Gelman and Rubin, 1992). For each chain we sampled the MCMC for at least 40,000 iterations, after at least 3,000 tuning samples.

5 Results

5.1 Simulation Study

Generally, estimator bias and error were low with the exponential model, and coverage was nominal (93.4% - 97.0%; Fig. 1; Appendix ?). However, estimates of r were imprecise (RMSE between 0.020 and 0.025; relative RMSE between 413% and 482% for non-zero true r) and biased low (between -0.008 and -0.005; relative bias between -151% and -101% for non-zero true r) when the true value of Λ was low (1). Simulations of the Ricker-logistic model also generally performed well (Fig. 2; Appendix ?), except when the true value of r was low (0.005). In this case the estimates of r and K were inaccurate (relative RMSE between 87.4% and 2091.8%), biased high (between 65.4% and 198.9%), and had low coverage (between 77.6% and 94.3%). In other cases for the Ricker-logistic model, relative RMSE was between 6.7% and 55%, bias was between -6.4% and 5.8%, and coverage was between 91.9% and 96.4%. All three cases simulated for the Ricker-logistic + immigration model performed fairly well (Fig. 3; Appendix ?; relative RMSE between 7.2% and 62.9%, bias between -3.5% and 3.3%, and coverage between 93.2% and 96.4%).

5.2 Analysis of Breeding Bird Survey Data

The negative binomial distribution was strongly supported for ovenbird initial abundance over the Poisson and zero-inflated Poisson (Table 2A). Even compared to the Poisson, there was no evidence to support a zero-inflation factor for this species. The best supported model for p was additive effects of wind speed and first run (Table 2B, model B.1). First run and increasing wind speeds both decreased p. All dynamics models with immigration were better supported than models without immigration (Table 2C); the best supported of these was the Ricker-logistic + immigration. The best supported model of those without immigration was the Gompertz-logistic, and the autoregressive and the constant model had the least support.

Estimates for the top ranked model for ovenbird were similar when run in the Bayesian framework, except that the estimate of r more than halved (from 0.026 ± 0.006 to 0.011 ± 0.005 [for Bayesian model estimates we present mean and SD]). When random observer effects were added, estimates for Λ and K increased dramatically (from 31.6 ± 4.9 to 42.5 ± 7.3 and from 56.2 ± 18.2 to 101.8 ± 21.1, respectively), and the estimate for r was intermediate (0.018 ± 0.006). The estimate of the intercept for p (on the logit scale) dropped from -1.5 ± 0.1 to -2.0 ± 0.1, and the estimate of σ_p was 0.35 ± 0.03. Gelman and Rubin diagnostics and visual examination of the chain trajectory and density plots provided some evidence for a lack of convergence in estimates of the intercept for p for all Bayesian models ran.

There was slightly more support for the ZIP distribution for initial abundance of golden-winged warbler than for the negative binomial; both were strongly supported over the Poisson (Table 3A). The best supported model for p was an effect of first run (Table 3B, model B.1). The best supported dynamics model was exponential (Table 3C, model C.1); the estimate of r from this model was -0.058 ± 0.017 (SE). There was no support for immigration added to the exponential or autoregressive models (Table 3C, models C.4 and C.6). However, the Gompertz-logistic + immigration and Ricker-logistic + immigration models were supported over the corresponding models without immigration (Table 3C, models C.4, C.5, C.7, and C.8), despite low estimates of ι from these models (0.003 ± 0.003 and 0.003 ± 0.002, respectively). Because of the closeness of rankings for the ZIP and negative binomial distributions for golden-winged warbler, we also ran the subsequent models with the negative binomial initial

abundance. Rankings of subsequent models were similar, but with a p covariate (first) the negative binomial distribution outranked the ZIP.

Estimates for the top ranked model for golden-winged warbler were similar when run in the Bayesian framework. When random observer effects were added, the estimate for Λ increased dramatically (from 22.4 ± 7.6 to 55.5 ± 30.9). The estimate of the intercept for p (on the logit scale) dropped from -3.5 ± 0.2 to -5.6 ± 1.1, and the estimate of σ_p was 1.7 ± 0.7. Adding zero-inflation to the dynamics (as well as the initial abundance) has no effect for exponential models, because populations that started at 0 would stay at 0 in any case. Therefore, we tested zero-inflated dynamics on the Exponential + Immigration model. Adding zero-inflation to the dynamics increased the estimate of from 0 to 0.091 ± 0.049, but had only minor effects on the other parameters. Gelman and Rubin diagnostics and visual examination of the chain trajectory and density plots provided evidence for a lack of convergence in estimates of Λ for all Bayesian models ran, and for most parameters when random effects were included.

Estimated detection probabilities were generally low. The estimated probability of detecting an ovenbird in the top model (Table 2, model C.1) varied between 0.157 ± 0.014 and 0.184 ± 0.015, depending on wind speed and whether the observer had run that route before. The estimated probability of detecting a golden-winged warbler went from 0.013 ± 0.006 for first time observers to 0.028 ± 0.008 for repeat observers for the top model (Table 3, model C.1). Accounting for random observer effects decreased average detection probability for both species.

For both species, constant dynamics models estimated very high survival probabilities ($\omega = 1 \pm 1.3\text{e-}05$ for ovenbird and 0.935 ± 0.011 for golden-winged warbler). The autoregressive and autoregressive + immigration models estimated very low survival probabilities for ovenbird ($\omega = 0.058 \pm 0.046$ and 0.026 ± 0.060, respectively), but not for golden-winged warbler ($\omega = 0.715 \pm 0.288$ for both models).

6   Discussion

Our work has highlighted the limitations of classical state-space models as applied to ecological time series data, and we have demonstrated how a class of open population N-mixture models proposed by Dail and Madsen (2011) overcomes these limitations. We extended their model in several important ways to accomodate common features of ecological datasets, including sparse counts, zero-inflation, demographic stochasticity, and random variation in observation error. We also demonstrated how many of the objectives of conventional state-space modeling can be accomplished within this expanded framework. For example, one of the primary aims of our paper was to demonstrate how classical population growth models can be embedded in the DM model. Although we view this as an important connection to make between the two different classes of state-space models, we believe that such population growth models are more phenomenological than mechanistic, and this runs counter to the motivation for the DM model. However, estimating demographic parameters from count data is an ambitious goal, and the required assumption will not be valid in many cases, especially when immigration and emigration occur. This was supported by the unrealistic estimates of vital rates reported here and by the lack of support for the mechanistic models relative to the population growth models.

One strategy for adhering to the original formulation of the model that included survival and recruitment parameters would be to use either prior information or additional data. For example, in a Bayesian analysis existing estimates of demographic parameters could be used as informative priors, which might make it possible to seper-

ate the effects of movement versus births and deaths. Alternatively, ecologists could combine count data with data from, for example, capture-recapture data. Models that are fitted to count data and demographic data are often referred to as integrated population models (IPM; Besbeas et al., 2002; Buckland et al., 2004; Schaub et al., 2007) and we believe that a DM model could work well in this context. In fact, the DM model could be viewed as a specific case of the IPM model proposed by Buckland et al. (2004). However, we caution that when count data are affected by movement and vital rates, it would be unwise to ignore the movement processes.

Although these integrated population models may be viewed as the gold standard in state-space modeling, ecologists are not always so fortunate to have direct information about vital rates, especially at large spatial scales. Rather, count data are much more common, and are produced by many of the largest monitoring programs in the world, such as the North American Breeding Bird Survey (BBS; Robbins et al., 1986). In the absence of direct information about demographic parameters, and when the original assumptions of the model do not hold, the model can still be used for important purposes such as predicting future population size and changes in species distributions.

[paragraph on random effects]

Another important benefit of this class of models is that it can be readily implemented using frequentist or Bayesian methods by ecologists lacking skills in computer programming and advanced statistics. We have included an appendix with extensive code to simulate and fit many of the extensions discussed in this paper. In spite of the new extensions we have proposed, several aspects of the model could be improved. First, the precision with which the parameters of the state process can be estimated ultimately depends upon how well detection probability is estimated. When there is only a single survey per primary period, the information about detection probability comes from deviations from the parametric assumptions about population dynamics. Thus, without direct information about detection probability, the estimates will be determined by the model's parametric assumptions. Furthermore, properly modeling detection probability can involve account for nuances such as difference among individuals and probabilities of being available for detection (Nichols et al., 2009).

Fortunately, it is straight-forward to incorporate direct information about detection probability and we recommend that this be done whenever possible. The original method for proposed in the original paper was to collected replicated counts within the primary periods during a period in which the populations could be assumed to be closed. A robust design could be used to combine multiple surveys per primary period to increase the precision of the estimates. We envision that multiple other options are available as well, such as removal, time of detection, and distance modeling ([cites]). These could be accomplished by extending the open population N-mixture model in exactly the same way as the closed population version has been extended (e.g., Royle et al., 2004).

Our emphasis was on increasing the practical utility of this class of models, and so we avoided several conceptually-interesting extensions that we belive would be computationally prohibitive in many cases. Nonetheless, we will discuss one—spatially-explicit models of immigration. In our models immigration is currently modeled as independent of population sizes in other sites. Several alternatives suggest themselves if we think about movement in a metapopulation context ([cite]): immigration depending on total or mean abundance across sites the previous time step; immigration depending on abundance in nearby sites only; and immigration depending on abundance at sites as a function of their distance from the receiving site (LOTS OF CITATIONS). These models would be based on the assumptions that either the study sites spatially cover the whole range of the metapopulation or the annual changes in

the populations sampled are representative of a larger metapopulation. Initial tests suggest that it would be possible to fit some or all of these models, at least in the Bayesian framework.

[simulation results discussion]

We have presented a test case for these models using data from the BBS for two species. We demonstrate that these models can be used to model and estimate initial abundance, detection probability, and density-independent and dependent functions for population dynamics. We tested these models in both the classical and Bayesian frameworks and found strengths and weaknesses of each approach. The Bayesian analyses permit more flexibility and allow the incorporation of random observer effects and zero-inflated dynamics. Our results suggest ignoring variation between observers can lead to underestimation of initial abundance and equilibrium population sizes. On the other hand, our Bayesian analyses did have convergence problems, particularly for the species (golden-winged warbler) with sparser data. It's likely that poor model fits are related to the low estimates of detection probability, which in turn are probably caused by the large 400 m radius used for BBS point counts. Again, we believe that direct information on detectability (such as repeated visits within a season) would greatly improve the fit of these models in both frameworks. [Alternatively, could put discussions of our results where they fit in by subject area, rather than separately. For instance, could discuss BBS population dynamics model selection in population models paragraph, BBS Bayesian vs. frequentist strengths and weakness in the Bayesian paragraph (currently not written), and golden-winged warbler ZIP results in ZIP paragraph.]

The modeling framework we described can be used to address many pressing issues in ecology and conservation biology. For example, it allows for inference about the effects of climate change on either explicit demographic parameters or in derived parameters such as population growth rate. Furthermore, in addition to assessing past climate change on population parameters, projecting populations under future climate scenarios is also possible. Thus, we expect this modeling methodology can be used to make quantiative assessments of species vulnerability to climate change and other important human-induced drivers of population dynamics.

7 Acknowledgements

References

Alldredge, M., K. Pollock, T. Simons, J. Collazo, S. Shriner, and D. Johnson, 2007. Time-of-detection method for estimating abundance from point-count surveys. *The Auk* **124**:653–664.

Besbeas, P., S. Freeman, B. Morgan, and E. Catchpole, 2002. Integrating mark–recapture–recovery and census data to estimate animal abundance and demographic parameters. *Biometrics* **58**:540–547.

Bjørnstad, O. and B. Grenfell, 2001. Noisy clockwork: time series analysis of population fluctuations in animals. *Science* **293**:638–643.

Bjørnstad, O., R. Ims, and X. Lambin, 1999. Spatial population dynamics: analyzing patterns and processes of population synchrony. *Trends in Ecology & Evolution* **14**:427–432.

Buckland, S., K. Newman, L. Thomas, and N. Koesters, 2004. State-space models for the dynamics of wild animal populations. *Ecological modelling* **171**:157–175.

Campbell, M. and C. M. Francis, 2011. Using stereo-microphones to evaluate observer variation in north american breeding bird survey point counts. *The Auk* **128**:303V–312.

Dail, D. and L. Madsen, 2011. Models for estimating abundance from repeated counts of an open metapopulation. *Biometrics* **67**:577–87.

de Valpine, P. and A. Hastings, 2002. Fitting population models incorporating process noise and observation error. *Ecological Monographs* **72**:57–76.

Dennis, B., J. Ponciano, S. Lele, M. Taper, and D. Staples, 2006. Estimating density dependence, process noise, and observation error. *Ecological Monographs* **76**:323–341.

Dennis, B. and M. Taper, 1994. Density dependence in time series observations of natural populations: estimation and testing. *Ecological monographs* **64**:205–224.

Diefenbach, D., D. Brauning, J. Mattice, and F. Thompson III, 2003. Variability in grassland bird counts related to observer differences and species detection rates. *The Auk* **120**:1168–1179.

Fiske, I. and R. Chandler, 2011. unmarked: An r package for fitting hierarchical models of wildlife occurrence and abundance. *Journal of Statistical Software* **43**:1–23.

Gelman, A. and D. B. Rubin, 1992. Inference from iterative simulation using multiple sequences. *Statistical Science* **7**:457V–472.

Hart, E. and N. Gotelli, 2011. The effects of climate change on density-dependent population dynamics of aquatic invertebrates. *Oikos* **120**:1227–1234.

Hatfield, J., M. Reynolds, N. Seavy, and C. Krause, 2012. Population dynamics of hawaiian seabird colonies vulnerable to sea-level rise. *Conservation Biology* .

Jamieson, L. and S. Brooks, 2004. Density dependence in north american ducks. *Animal Biodiversity and Conservation* **27**:113–128.

Kery, M., R. Dorazio, L. Soldaat, A. Van Strien, A. Zuiderwijk, and J. Royle, 2009. Trend estimation in populations with imperfect detection. *Journal of Applied Ecology* **46**:1163–1172.

Lele, S., M. Taper, and S. Gage, 1998. Statistical analysis of population dynamics in space and time using estimating functions. *Ecology* **79**:1489–1502.

Link, W. and J. Nichols, 1994. On the importance of sampling variance to investigations of temporal variation in animal population size. *Oikos* **69**:539–544.

Link, W. and J. Sauer, 2002. A hierarchical analysis of population change with application to cerulean warblers. *Ecology* **83**:2832–2840.

MacKenzie, D., J. Nichols, J. Royle, K. Pollock, L. Bailey, and J. Hines, 2006. Occupancy estimation and modeling: inferring patterns and dynamics of species occurrence. Academic Press.

May, R., 1975. Biological populations obeying difference equations: stable points, stable cycles, and chaos. *Journal of Theoretical Biology* **51**:511–524.

Nadeem, K. and S. Lele, 2011. Likelihood based population viability analysis in the presence of observation error. *Oikos* .

Nichols, J., L. Thomas, and P. Conn, 2009. Inferences about landbird abundance from count data: recent advances and future directions. *Modeling demographic processes in marked populations* pages 201–235.

O'Hara, R. and D. Kotze, 2010. Do not log-transform count data. *Methods in Ecology and Evolution* **1**:118–122.

Plummer, M., 2003. Jags: A program for analysis of bayesian graphical models using gibbs sampling. In *Proceedings of the 3rd International Workshop on Distributed Statistical Computing (DSC 2003). March*, pages 20–22.

Plummer, M., 2011. rjags: Bayesian graphical models using MCMC. R package version 3-5.

Polansky, L., P. De Valpine, J. Lloyd-Smith, and W. Getz, 2009. Likelihood ridges and multimodality in population growth rate models. *Ecology* **90**:2313–2320.

R Development Core Team, 2012. R: A Language and Environment for Statistical Computing. R Foundation for Statistical Computing, Vienna, Austria. ISBN 3-900051-07-0.

Ricker, W., 1954. Stock and recruitment. *Journal of the Fisheries Board of Canada* **11**:559–623.

Robbins, C., D. Bystrak, and P. Geissler, 1986. The breeding bird survey: its first fifteen years, 1965-1979. Technical report, US Fish and Wildlife Service.

Royama, T., 1977. Population persistence and density dependence. *Ecological Monographs* pages 1–35.

Royle, J., 2004. N-mixture models for estimating population size from spatially replicated counts. *Biometrics* **60**:108–115.

Royle, J. A., D. K. Dawson, and S. Bates, 2004. Modeling abundance effects in distance sampling. *Ecology* **85**:1591–1597.

Sæther, B. and S. Engen, 2002. Pattern of variation in avian population growth rates. *Philosophical Transactions of the Royal Society of London. Series B: Biological Sciences* **357**:1185–1195.

Sauer, J. and W. Link, 2011. Analysis of the north american breeding bird survey using hierarchical models. *The Auk* **128**:87–98.

Sauer, J., B. Peterjohn, and W. Link, 1994. Observer differences in the north american breeding bird survey. *The Auk* pages 50–62.

Schaub, M., O. Gimenez, A. Sierro, and R. Arlettaz, 2007. Use of integrated modeling to enhance estimates of population dynamics obtained from limited data. *Conservation Biology* **21**:945–955.

Schoener, T. and D. Spiller, 1992. Is extinction rate related to temporal variability in population size? an empirical answer for orb spiders. *American Naturalist* pages 1176–1207.

Shenk, T., G. White, and K. Burnham, 1998. Sampling-variance effects on detecting density dependence from temporal trends in natural populations. *Ecological Monographs* **68**:445–463.

Simons, T., M. Alldredge, K. Pollock, J. Wettroth, and A. Dufty Jr, 2007. Experimental analysis of the auditory detection process on avian point counts. *The Auk* **124**:986–999.

Turchin, P., 1990. Rarity of density dependence or population regulation with lags? *Nature* **344**:660–663.

Table 1: Changed parameter values, by series of simulations. We simulated 1000 sets of data each combination of parameter values for 100 sites over 40 years. We assumed that initial abundance (Λ) was Poisson distributed. For the exponential simulations we included all combinations of low, medium, and high Λ, growth rate (r), and detection probability (p). For the Ricker-logistic model simulations we used $\Lambda = 10$ and $p = 0.25$, and simulated low, medium, and high values of r and equilibrium density (K). For the Ricker-logistic + immigration dynamics model we fixed all parameters the same as the Ricker-logistic model (with $r = 0.05$ and $K = 10$) and simulated low, medium, and high values of immigration rate (ι).

| | Exponential Growth | | | Ricker-logistic | | Ricker-logistic + Immigration |
	Λ	r	p	r	K	ι
Low	1	-0.01	0.05	0.005	5	0.005
Med	5	0	0.25	0.05	10	0.05
High	10	0.005	0.5	0.1	20	0.5

Table 2: Model selection table for ovenbirds in Maryland and Virginia, 1966-2010. We present model name and number, number of parameters (Par.), and difference in Akaike's information criterion between each model and the top model of that set (ΔAIC). The first section compares models for initial abundance, the second for detection probability, and the third for dynamics.

Model	Par.	ΔAIC
A. Initial Abundance		
A.1. NB[$\Lambda(.)\alpha(.)$]Exponential[$r(.)$]$p(.)$	4	0
A.2. P[$\Lambda(.)$]Exponential[$r(.)$]$p(.)$	3	1262.7
A.3. ZIP[$\Lambda(.)\psi(.)$]Exponential[$r(.)$]$p(.)$	4	1264.7
B. Detection Probability		
B.1. NB[$\Lambda(.)\alpha(.)$]Exponential[$r(.)$]p(wind+1st)	8	0
B.2. NB[$\Lambda(.)\alpha(.)$]Exponential[$r(.)$]p(wind)	7	0.9
B.3. NB[$\Lambda(.)\alpha(.)$]Exponential[$r(.)$]p(1st)	5	5.0
B.4. NB[$\Lambda(.)\alpha(.)$]Exponential[$r(.)$]$p(.)$	4	6.4
C. Dynamics		
C.1. NB[$\Lambda(.)\alpha(.)$]Ricker-logistic+Immigration[$r(.)K(.)\iota(.)$]p(wind+1st)	10	0
C.2. NB[$\Lambda(.)\alpha(.)$]Gompertz-logistic+Immigration[$r(.)K(.)\iota(.)$]p(wind+1st)	10	8.4
C.3. NB[$\Lambda(.)\alpha(.)$]Exponential+Immigration[$r(.)\iota(.)$]p(wind+1st)	9	36.5
C.4. NB[$\Lambda(.)\alpha(.)$]Autoregressive+Immigration[$\gamma(.)\omega(.)\iota(.)$]$p$(wind+1st)	10	38.6
C.5. NB[$\Lambda(.)\alpha(.)$]Gompertz-logistic[$r(.)K(.)$]p(wind+1st)	9	192.8
C.6. NB[$\Lambda(.)\alpha(.)$]Ricker-logistic[$r(.)K(.)$]p(wind+1st)	9	195.1
C.7. NB[$\Lambda(.)\alpha(.)$]Exponential[$r(.)$]p(wind+1st)	8	271.3
C.8. NB[$\Lambda(.)\alpha(.)$]Autoregressive[$\gamma(.)\omega(.)$]p(wind+1st)	9	273.7
C.9. NB[$\Lambda(.)\alpha(.)$]Constant[$\gamma(.)\omega(.)$]p(wind+1st)	9	1856.7

Table 3: Model selection table for golden-winged warblers in Maryland and Virginia, 1966-2010. We present model name and number, number of parameters (Par.), and difference in Akaike's information criterion between each model and the top model of that set (ΔAIC). The first section compares models for initial abundance, the second for detection probability, and the third for dynamics.

| Model	Par.	ΔAIC
A. Initial Abundance		
A.1. ZIP[$\Lambda(.)\psi(.)$]Exponential[$r(.)$]$p(.)$	4	0
A.2. NB[$\Lambda(.)\alpha(.)$]Exponential[$r(.)$]$p(.)$	4	0.4
A.3. P[$\Lambda(.)$]Exponential[$r(.)$]$p(.)$	3	37.8
B. Detection Probability		
B.1. ZIP[$\Lambda(.)\psi(.)$]Exponential[$r(.)$]$p(1\text{st})$	5	0
B.2. ZIP[$\Lambda(.)\psi(.)$]Exponential[$r(.)$]$p(.)$	4	3.5
B.3. ZIP[$\Lambda(.)\psi(.)$]Exponential[$r(.)$]$p(\text{wind}+1\text{st})$	8	5.9
B.4. ZIP[$\Lambda(.)\psi(.)$]Exponential[$r(.)$]$p(\text{wind})$	7	9.3
C. Dynamics		
C.1. ZIP[$\Lambda(.)\psi(.)$]Exponential[$r(.)$]$p(1\text{st})$	5	0
C.2. ZIP[$\Lambda(.)\psi(.)$]Autoregressive[$\gamma(.)\omega(.)$]$p(1\text{st})$	6	1.7
C.3. ZIP[$\Lambda(.)\psi(.)$]Exponential+Immigration[$r(.)\iota(.)$]$p(1\text{st})$	6	2.0
C.4. ZIP[$\Lambda(.)\psi(.)$]Gompertz-logistic+Immigration[$r(.)K(.)\iota(.)$]$p(1\text{st})$	7	2.5
C.5. ZIP[$\Lambda(.)\psi(.)$]Gompertz-logistic[$r(.)K(.)$]$p(1\text{st})$	6	3.0
C.6. ZIP[$\Lambda(.)\psi(.)$]Autoregressive+Immigration[$\gamma(.)\omega(.)\iota(.)$]$p(1\text{st})$	7	3.7
C.7. ZIP[$\Lambda(.)\psi(.)$]Ricker-logistic+Immigration[$r(.)K(.)\iota(.)$]$p(1\text{st})$	7	4.2
C.8. ZIP[$\Lambda(.)\psi(.)$]Ricker-logistic[$r(.)K(.)$]$p(1\text{st})$	7	5.2
C.9. ZIP[$\Lambda(.)\psi(.)$]Constant[$\gamma(.)\omega(.)$]$p(1\text{st})$	6	12.5
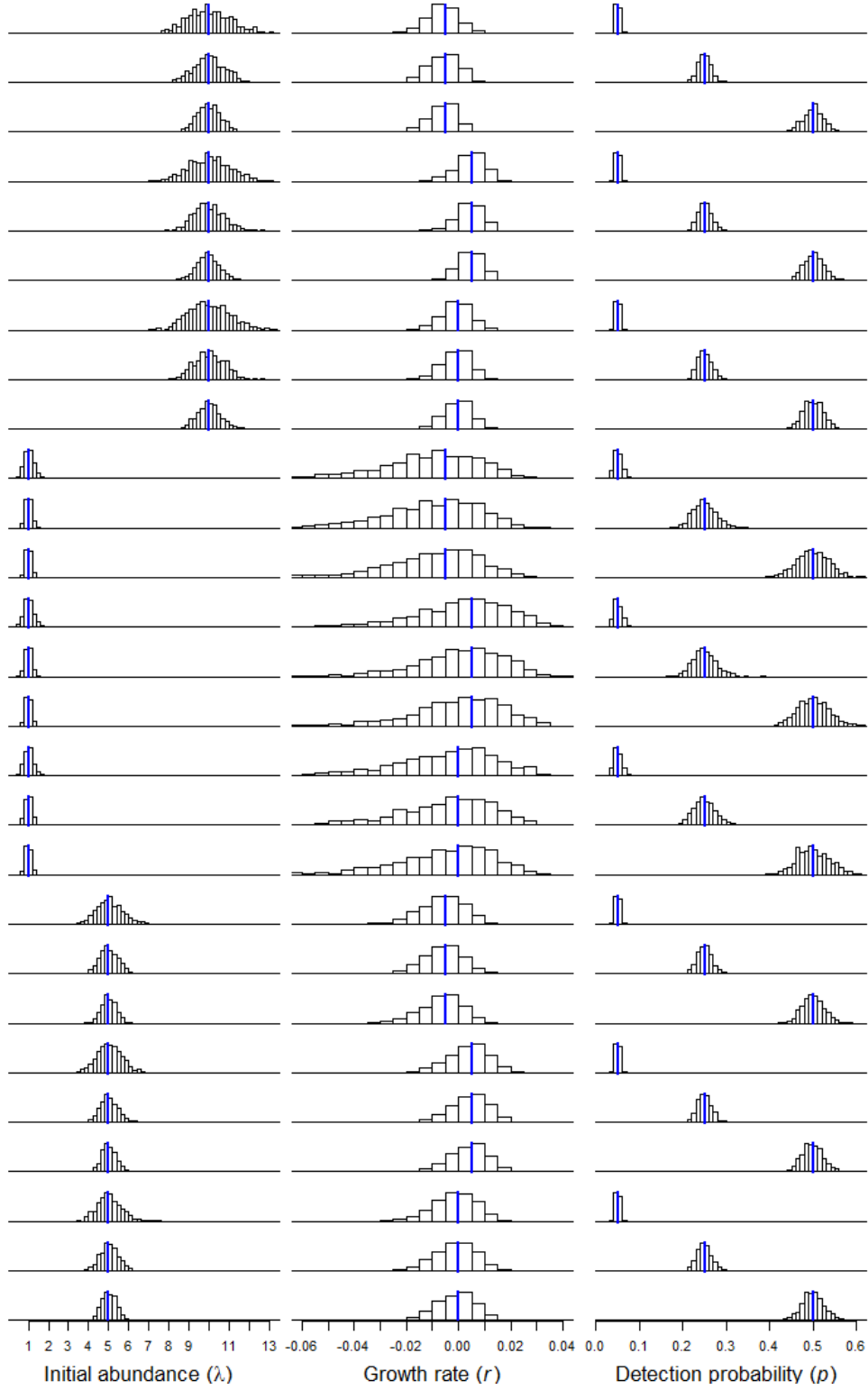
Figure 1: Histograms of 1000 parameter estimates for each of 27 simulation cases with exponential dynamics. The vertical lines are the data-generating values.
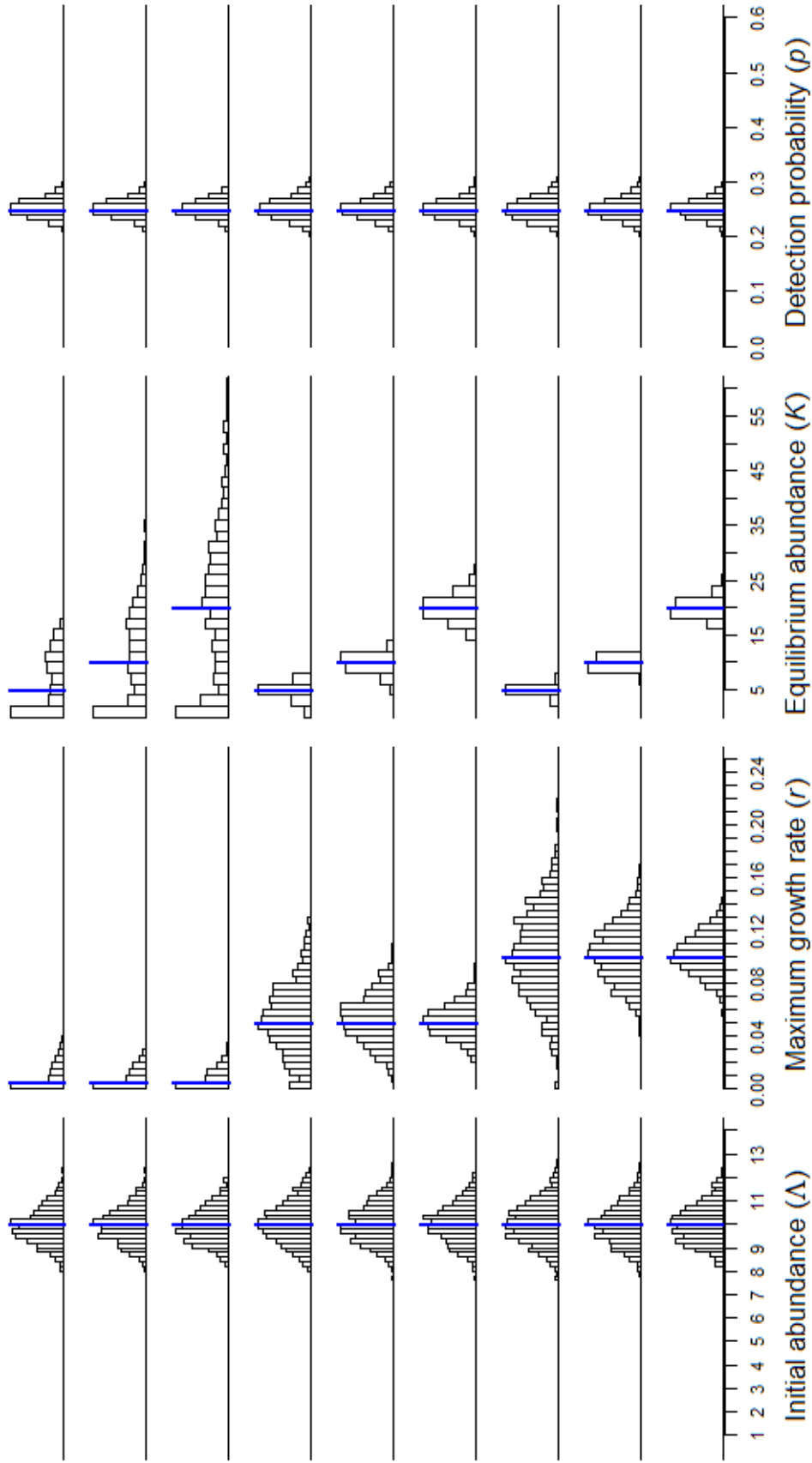
Figure 2: Histograms of 1000 parameter estimates for each of 9 simulation cases with Ricker-logistic dynamics. The vertical lines are the data-generating values.
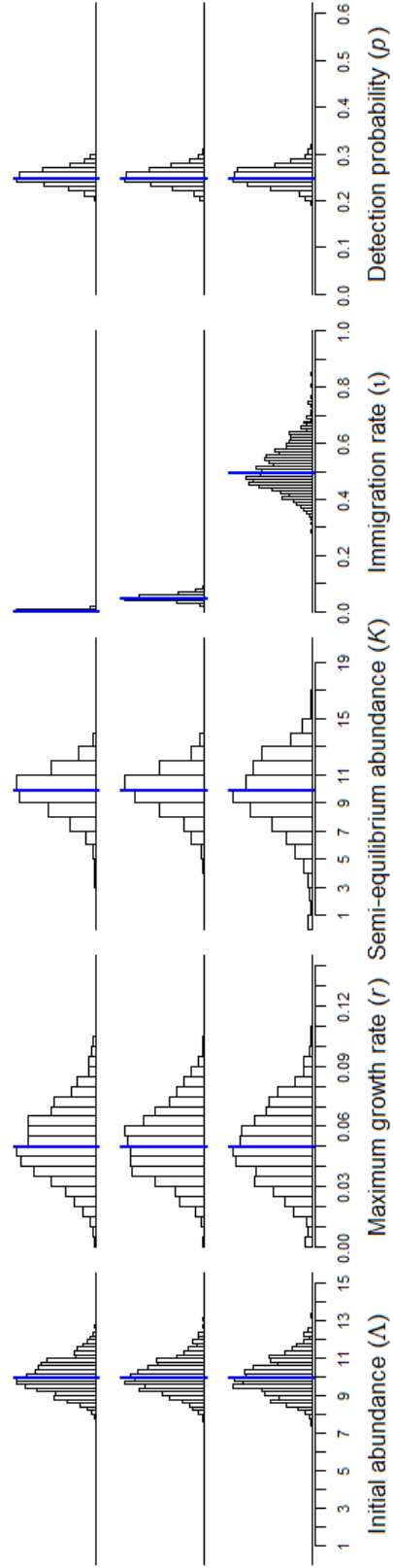
Figure 3: Histograms of 1000 parameter estimates for each of 3 simulation cases with Ricker-logistic + immigration dynamics. The vertical lines are the data-generating values.